Neurotoxicology 73 (2019) 100–111

Contents lists available at ScienceDirect

Neurotoxicology

journal homepage: www.elsevier.com/locate/neuro

Full Length Article

Ulmosides A: Flavonoid 6-C-glycosides from *Ulmus wallichiana* attenuates lipopolysacchride induced oxidative stress, apoptosis and neuronal death

Parul Gupta[a,b], Abhishek Singh[a,b], Shubhangini Tiwari[a], Amit Mishra[c], Rakesh Maurya[a], Sarika Singh[a,b,*]

[a] Toxicology and Experimental Medicine Division, CSIR-Central Drug Research Institute, Lucknow, 226031, UP, India
[b] Academy of Scientific & Innovative Research (AcSIR), India
[c] Cellular and Molecular Neurobiology Unit, Indian Institute of Technology Jodhpur, Rajasthan, 342011, India

ARTICLE INFO

Keywords:
Ulmus wallichiana
Neuroprotection
Antioxidative
Antiapoptotic

ABSTRACT

Extract of *Ulmus wallichiana* is being used as traditional medicine used for the treatment of fractured bones however the effect of its individual flavonols is not known. The present study was conducted to investigate the effect of its novel flavonol, (2S, 3S)-(+)-30, 40, 5, 7-tetrahydroxydihydroflavonol-6-C-b-D-glucopyranoside named as Ulmoside A (UA), on lipopolysaccharides (LPS) treated neurons. LPS treatment to neuronal cells caused significant cytotoxicity, reactive oxygen species generation, depletion in glutathione and mitochondrial impairment which were significantly inhibited with UA treatment. LPS treatment also caused significant translocation of cytochrome-c, decreased level of Bcl2, increased level of Bax and cleaved caspase-3 in neuronal cells reflecting the involvement of intrinsic apoptotic pathway in neuronal death which was attenuated with UA treatment. Since LPS is a well known pro-inflammatory agent it also offered the significant increase in proinflammatory cytokines (tumor necrosis factors-α & interleukin 1-beta) however, UA treatment did not exhibit significant inhibition against LPS induced inflammatory response. LPS also caused the augmented level of inducible nitric oxide synthase (iNOS) which was also not inhibited with co treatment of UA. We have also observed the significant DNA fragmentation and augmented level of cleaved Poly (ADP-Ribose) polymerase 1 after LPS treatment which was significantly reverted with UA treatment. Findings suggested that UA acts through mitochondria and exhibited its anti-oxidative and anti-apoptotic activities in neuronal cells while no significant anti-inflammatory activity and effect on iNOS were observed.

1. Introduction

Flavonoids are secondary metabolites of plants, fruits, vegetables and are known as the most common phytochemicals possessing multiple pharmacological effects. These secondary metabolites are potent antioxidant, free radical scavengers, and metal chelators (Agati et al., 2012; Brunetti et al., 2013). These also possess anticholinesterase (Bensouici et al., 2016; Stankov-Jovanović et al., 2015), antiaging (Wang et al., 2016; Davinelli et al., 2018), anti-inflammatory properties (Bose et al., 2017), and neuroprotective (Scotti and Scotti, 2015; Fernández-Moriano et al., 2016) activities. These could also suppress the activation of microglia (Lee et al., 2013; Dilshara et al., 2014) thus have interfering effects in inflammatory mechanisms mediated neuronal death in central nervous system (Venigalla et al., 2015; Apetz et al., 2014; Kim et al., 2013). Furthermore, these could cross the blood-brain barrier with chronic or acute administration thus have a direct effect on the brain, and could be used as a prophylactic agent to slow down the progression of neurodegenerative diseases like AD and PD (Plummer et al., 2016; Houghton and Howes, 2005; Kim et al., 2015a). The use of flavonoid-rich plant or food extracts exhibited the improvements in cognition function possibly by protecting vulnerable neurons through enhancing existing neuronal function or by stimulating neuronal regeneration (Vauzour et al., 2019).

U. wallichiana is a crucial traditional plant species of India which is medicinally used for treatment of bone fracture (Maurya et al., 2008; Swarnkar et al., 2011; Khan et al., 2013; Siddiqui et al., 2011; Sharan et al., 2010) however its neuroprotective effects are not yet known. Previously we have done the fractionation of ethanolic extract of stem bark of U. *wallichiana* and for the first time identified C-glycoside flavonoids as potential bone anabolic agents (Rawat et al., 2009). Ethanolic extract of *U. wallichiana* contains two new flavonoid C-glucosides, five known flavonoid C-glucosides and one new phenolic-C-glucoside.

* Corresponding author.
E-mail address: sarika_singh@cdri.res.in (S. Singh).

https://doi.org/10.1016/j.neuro.2019.02.017
Received 10 September 2018; Received in revised form 9 January 2019; Accepted 25 February 2019
Available online 08 March 2019
0161-813X/

The isolated novel flavonol (2S, 3S)-(+)-30, 40, 5, 7-tetrahydroxydihydroflavonol-6-C-b-D-glucopyranoside, named as ulmoside A (UA) is utilized in present study to evaluate its role against neuronal death.

Lipopolysacchride (LPS) induced neuronal death has been reported by us and others involving oxidative, apoptotic and inflammatory pathways (Ning et al., 2017; Fernandes et al., 2018; Verma et al., 2018a). LPS treatment to neurons caused mitochondrial dysfunction mediated oxidative stress induced neuronal apoptosis (Kim et al., 2015b; Chen et al., 2015; Kuwabara and Imajoh-Ohmi, 2004) which is also involved in AD and PD pathophysiology (Moreira et al., 2010). LPS induced neurotoxicity also involve the proteolytic enzymes and inflammatory cytokines that may further contributes to mitochondrial dysfunction and chronic neurodegenerative conditions as observed in AD and PD (Leuner et al., 2010; Winklhofer and Haass, 2010). Previously we have shown that LPS treatment to neuronal N2A cells caused oxidative stress, induction of inflammatory responses and caspase independent neuronal death. In glioma cells we have shown that LPS treatment caused DNA fragmentation involving translocation of mitochondrial endonuclease G and apoptosis inducing factors. In rat brain we have reported that LPS administration caused mitochondrial impairment mediated intrinsic neuronal apoptosis (Singh et al., 2010). Mitochondria mediated neuronal apoptosis involve the cytochrome-c translocation from mitochondria to cytosol and depleted level of anti-apoptotic protein Bcl-2 (Giorgio et al., 2005; Sarkar et al., 2003; Reed and Green, 1998; Biswas et al., 2016). Depleted level of Bcl-2 along with up regulated Bax may cause the increased level of cleaved caspase-3 and thus neuronal apoptosis. Since LPS exposure caused mitochondria mediated intrinsic apoptosis in neurons and flavonoids could offer antioxidative and antiapoptotic pathway, therefore LPS was used in present study to cause neuronal death and effect of UA was investigated. The prime focus of present study is to evaluate the effect of UA on the LPS induced alterations in neuronal cells assessing its anti-oxidative, anti-inflammatory and anti-apoptotic activities.

2. Experimental procedures

2.1. Chemicals

Bovine serum albumin, dichloro fluorescein diacetate (DCF-DA), dihydro ethidium, disodium hydrogen phosphate, dimethyl sulfoxide (DMSO), ethidiumbromide,glucose,4-(2-hydroxyethyl)-1-piperazine ethane sulfonic acid (HEPES), 3-(4,5-dimethylthiazol-2-yl)-2,5- diphenyl tetrazolium bromide dye (MTT), low-melting-point (LMP) agarose, magnesium chloride, NADH, propidium iodide, RNase, sodium bicarbonate, sodium pyruvate and Tris buffer were procured from Sigma (StLouis MO,USA). Dulbecco's modified Eagle's medium (DMEM), fetal bovine serum (FBS), Trizol, Ham's F12medium, and penicillin–streptomycin were purchased from Invitrogen (SanDiego, CA, USA). Laboratory chemicals such as copper sulfate, calcium chloride, Folin–Ciocalteu reagent, potassium chloride, sodium carbonate, sodium chloride, sodium dihydrogen phosphate, sodium hydroxide, sodium potassium tartarate and ethylenediamine tetraacetic acid (EDTA) were procured from company Sigma, USA. Rabbi polyclonal anti-caspase-3 Ab, mouse anti-β-actin Ab, rabbit polyclonal anti-Bax Ab, rabbit polyclonal anti-Bcl-2 Ab, anti-mouse FITC-conjugated and anti-mouse and anti-rabbit HRP-secondary Abs were procured from Sigma.

2.2. Cell culture and treatments

The mouse neuroblastoma N2A cell line was procured from the National Center of Cell Sciences, Pune, India and maintained at the Central Drug Research Institute. Cells were cultured in a mixture of DMEM and F12 (1:1) media supplemented with 10% FBS at 37^0C and 5% CO_2 using standard cell culture methods. Treatment was given with various concentrations of LPS (10, 50, and 100 μg/ml) for 24 h. Co treatment with Ulmoside A (UA, 0.1 & 1μM) was also given to evaluate its effects in cells for 24 h. All the experiments were repeated for three to five times and conducted with triplicates of each set each time.

2.3. Mitochondrial dehydrogenase activity (MTT assay)

The activity of mitochondrial dehydrogenase was evaluated by utilizing MTT dye following the method as reported in Gupta et al. (2014). Briefly, cells were counted by hemocytometer and 1×10^5 cells were seeded in 96 well plates and treated with LPS and / or LPS with UA for 24 h. After treatment the cells were incubated with MTT dye for 2 h at 37^0C. The culture medium was then removed and 200 μl DMSO was added. The blue-colored formazan was dissolved in DMSO. The absorbance of formazan was read at 550 nm wavelength by a spectrophotometer (Gen5, BioTek) with reference wavelength of 630 nm. Observed optical density is directly proportional to cell viability.

2.4. Lactate dehydrogenase (LDH) assay

Cytotoxicity was assessed by release of LDH enzyme in to the culture medium. It is a soluble enzyme located in the cytosol and released in to the adjacent culture medium upon cell lysis. LDH activity in culture medium can subsequently be utilized as a marker of cell death. The 2×10^6 cells were seeded in six-well plates and treated with different concentrations of LPS and / or LPS with UA. After treatment the culture medium was saved for LDH assay and cells were processed for comet assay. The amount of protein in every samples was evaluated by Lowry's method (Lowry et al., 1951). LDH estimation was done by the method described by Wroblewski and Ladue (1955). A reaction mixture was prepared by adding phosphate buffer (0.1 M NaH_2PO_4 and 0.1 M Na_2HPO_4, pH 7.2), sodium pyruvate (1.5 mM) and 100 μg of protein. This mixture was incubated at 37^0C for 30 min and the reaction was initiated with the addition of 0.5 mM NADH. Change in absorbance was estimated by a spectrophotometer (BioTek, Winooski, USA) at wavelength 340 nm for two minutes at an interval of 15 s. Enzyme activity was calculated as substrate utilized by LDH per minute / mg of protein.

2.5. Mitochondrial membrane potential

Estimation of mitochondrial membrane potential (MMP) was estimated via the fluorescent dye rhodamine 123 (R123) as described by Hail and Lotan (2000). R123 is sequestered in the mitochondria of viable cells due to high negative electric potential over the mitochondrial inner membrane. Cells (1×10^5) were seeded in 96 well plates. After treatment, the culture medium was removed and R123 was added to cells at a final concentration of 10 μg/ml in Krebs Ringer buffer and incubated for 30 min at 37°C. After incubation the fluorescence was recorded by a fluorimeter (Varian) with excitation at 508 nm and emission at 530 nm.

2.6. Reactive oxygen species

Generation of reactive oxygen species (ROS) was estimated by using DCF-DA dye. DCF-DA assay was performed according to the protocol described by Ryu et al. (2003). Briefly, 1×10^5 cells were seeded in 96 well plates and after treatment the cells were washed with Krebs Ringer buffer and incubated with DCF-DA for 90 min. After incubation the fluorescence was measured by fluorimeter (Varian) with excitation at 485 nm and emission at 520 nm.

2.7. Glutathione estimation

Reduced glutathione (GSH) as a marker of oxidative stress was estimated by procedure reported by Javed et al. (2012) with slight modifications. After treatment the cells were washed, collected and

sonicated in 0.1 M sodium phosphate buffer (PB). Supernatant was mixed with 4% trichloroacetic in 1:1 proportion (v/v) and incubated for 1 h at 4°C. Then incubated samples were centrifuged at 4000× *g* for 10 min at 4°C and supernatant is used to set the reaction mixture. Reaction mixture was prepared by adding 10 µl of supernatant, 1 mM DTNB and 0.1 M PB (pH 7.4) in total volume of 200 µl. The absorbance of yellow coloured product was quickly read at wavelength of 412 nm utilizing ELISA plate reader (BIO-TEK Instruments). The GSH concentration was extrapolated by utilizing standard curve plotted by optical density of the known concentration of GSH standard. Results were expressed as GSH µg/mg of protein.

2.8. mRNA expression by reverse transcriptase -PCR

RNA was isolated from cells utilizing trizol reagent as prescribed by the manufacturer. Concentration and purity of the RNA were determined spectrophotometrically (BioTek). 2 µg of total RNA was utilized to prepare cDNA by high capacity cDNA reverse transcription kit based on protocol in 20 µl reaction volume. The cDNA was amplified separately with specific primers for β-actin, TNF-α and IL-1β using PCR master mix in 96-well Veriti thermal cycler (Applied Biosystems). The primers for β-actin forward 5′-GTCGTACCACTGGCATTGTG-3′and β-actin reverse 5′-CTCTCAGCTGTGGTGGTGAA-3′(Tm 56^{0}C) and TNF-α forward 5′-AGGGAGAACAGCAACTCCAGAACA-3′and TNF-α reverse 5′-TGCCAGTTCCACATCTCGGATCAT-3′(Tm 59^{0}C) and IL-1β forward 5′-AGCAGCTTTCGACAGTGAGGAGAA-3′and IL-1β reverse 5′-TCTCCACAGCCACAATGAGTGACA-3′ (Tm 58°C) (IDT) produced amplified fragments of lengths 181 bp, 105 bp and 161 bp respectively. The polymerase chain reaction mixture was amplified in a DNA thermal cycler (Applied Biosystems) through 35 cycles. The PCR products were identified by electrophoresis on a 2% agarose gel containing ethidium bromide. Images were captured by an UVI gel documentation system and intensity was measured by Image *J* software.

2.9. Western blotting

The total lysate and cellular fractions were isolated from different protocols as previously published and briefly described below. After treatment the cells were collected in culture medium by scrapper and centrifuged at 3000 × rpm for 15 min at 4°C (Gupta et al., 2014). Cells were washed with phosphate buffer saline (PBS) and collected by centrifugation. To obtain the total lysate the pellet was sonicated in lysis buffer containing 200 mM HEPES (pH 7.4), 250 mM sucrose, 1 mM dithiothreitol, 1.5 mM $MgCl_2$, 10 mM KCl, 1 mM EDTA, 1 mM EGTA, 0.1 mM phenylmethylsulfonyl fluoride, protease inhibitor cocktail, and 1% NP-40 and then centrifuged at 1000 × *g* for 15 min at 4°C. After centrifugation, the supernatant was taken as the total lysate. Protein content was determined by the Lowry method and loaded on gel to detect the signal. The mitochondrial and cytosolic fractions of cells were obtained by the protocol as reported by us previously (Biswas et al., 2016). Briefly, after treatment cells were collected and washed with PBS and pellet was resuspended in isolation buffer (320 mM sucrose, 1 mM potassium EDTA, 10 mM Tris − HCL (pH-7.4)). Cells were homogenize by using micro pestle with 20–30 strokes, than the lysate was centrifuged at 1500 × *g* for 10 min, supernatant (S1) was kept on ice and repeat the process, collect the other supernatant (S2), combine supernatant (S1 + S2) and centrifuged it at 17,000 × *g* for 11 min at 4°C. Use supernatant as cytosolic fraction and dissolve the pellet in isolation buffer use this as mitochondrial fraction. The samples were loaded on an SDS–polyacrylamide gel and blotted on to a polyvinylidenedifluoride membrane. The membrane was blocked with 5% BSA, washed with PBS-tween (0.1%) and incubated with primary antibody β-actin (1:2000), iNOS (1:1000), caspase-3, Bax, Bcl-2, PARP-1, cytochrome–c (1:500) overnight. After incubation with primary antibody, the membranes were washed and incubated with appropriate HRP conjugated secondary antibody (1:2000) for 1 h at room temperature. Signals were developed under ChemiDoc XRS + (Bio-Rad) by using femto lucent plus HRP (G-Biosciences). Mean intensity of bands was determined and normalized by β-actin using ImageJ software (NIH, USA) and bar diagram was plotted.

2.10. Annexin V/PI staining by flow cytometry

Apoptosis was evaluated by Annexin V-FITC staining kit based on the manufacturer's protocol. Cells were treated with LPS (100 µg/ml) as well as LPS + UA for 24 h. After treatment, the cells were trypsinized and washed with PBS. The 1 × 10^6 cells were gently resuspended in 1 × binding buffer and incubated with 1.25 µl of Annexin V-FITC for 15 min in dark. After that, 10 µl of propidium iodide was added and reaction mixture was incubated for 10 min at room temperature in dark. Fluorescence was observed by flow cytometer (BD FACS Calibur) and analyzed by Cell Quest Pro software (BD).

2.11. Comet assay/single-cell gel electrophoresis

This assay was performed according to the method by (Singh et al., 2011) with slight modifications. Briefly, 0.8% low melting point (LMP) agarose was prepared in saline and maintained at 40^{0}C to prevent its solidification. Cells were treated with various concentrations of LPS and/or LPS + UA. After treatment, the cells were trypsinized and washed with PBS and finally 1 × 10^5 cells were gently mixed with 250 µl of 0.8% LMP agarose. The resulting suspension was layered onto the frosted side of fully frosted slides. The slides were placed on ice for approximately 5 min to allow the agarose to solidify. Subsequently the slides were immersed in the lysis solution for 1 h to eliminate all non-nuclear components. The slides were then further immersed in alkaline buffer (pH-13) for 20 min to allow DNA unwinding and conversion of alkali labile sites to single strand breaks. Next, electrophoresis was conducted for 30 min at 15 V and 200 mA, i.e., at the rate of 0.6 V/cm, using a compact power supply. The slides were then gently washed with 0.4 M tris (pH 7.5) to remove the alkali and detergents. All the slides were placed in a humid chamber until staining to prevent the gel from drying. The cells were stained with PI (20 µg/ml) and observed under a fluorescence microscope (Nikon Eclipse TE2000S) and the images were captured using a digital camera. About 60–80 images per slide per sample were captured from different imaging fields and analyzed. The olive tail moment (OTM) parameter was analyzed using CASP software.

2.12. Statistical analysis

Data were analyzed by one way analysis of variance (ANOVA) and the difference between control cells and treated cells was analyzed by post hoc Newman–Keuls multiple comparison test. Values are expressed as the mean ± standard error of the mean. p values less than 0.05 were considered statistically significant.

3. Results

3.1. Cell viability (MTT Assay)

LPS treatment in N2A cells for 24 h caused significantly ($p < 0.001$) decreased mitochondrial dehydrogenase activity as estimated by MTT assay (Fig. 1). The MTT reduction in the control cells was 0.69 ± 0.01 whereas the MTT reduction in LPS treated cells was 0.69 ± 0.01, 0.51 ± 0.01 and 0.47 ± 0.01 at 10, 50 and 100 µg/ml concentrations of LPS respectively. The MTT reduction in UA per se treated cells was 0.65 ± 0.01 and 0.60 ± 0.01 at 0.1 and 1 µM which was not significantly different from control values. Co treatment of UA with LPS offered significant ($p < 0.001$) protection against LPS induced decreased MTT reduction with combination of both 0.1 and 1 µM concentrations of UA. The MTT reduction in LPS + UA treated cells was 0.86 ± 0.02, 0.6 ± 0.16 and 0.56 ± 0.03 with 0.1 µM concentration

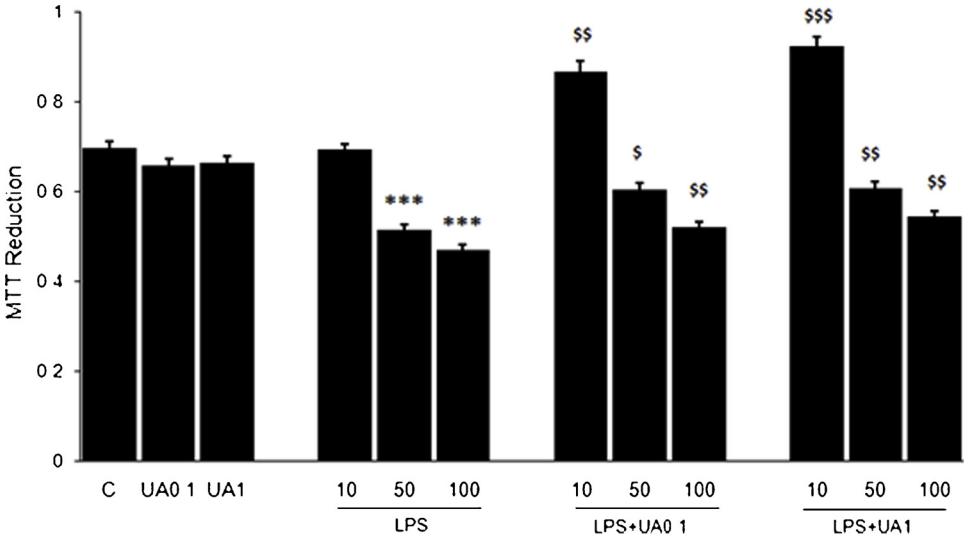

Fig. 1. Bar diagram illustrating the cell viability (MTT reduction) in N2A cells after 24 h of treatment. LPS caused a significant decrease in cell viability. Ulmoside A (UA) showed significant protection against LPS induced adverse effects. Data are expressed as mean ± SEM, analyzed by one way ANOVA post hoc Newman Keuls multiple comparison test. ***p < 0.001 control vs. LPS and $p < 0.05, $$p < 0.01, $$$p < 0.01 LPS vs. LPS + UA.

of UA while with 1 μM concentration of UA the MTT reduction was 0.92 ± 0.02, 0.6 ± 0.01 and 0.55 ± 0.01 at 10, 50 and 100 μg/ml concentrations of LPS respectively (Fig. 1).

3.2. Cell cytotoxicity (LDH Assay)

In control cells, the LDH activity was 0.67 ± 0.10 per minute / mg of protein while in LPS treated cells, the LDH activity was 1.98 ± 0.31, 2.71 ± 0.21 and 3.50 ± 0.21 per minute / mg of protein at 10, 50 and 100 μg/ml concentrations of LPS respectively which was significantly ($p < 0.001$) increased in comparison to control cells. The LDH activity in UA per se treated cells was 0.92 ± 0.13 per minute/mg of protein. Co-treatment of UA at both 0.1 and 1 μM concentrations with LPS offered significant ($p < 0.001$) reduction in LPS induced increased LDH activity at 50 and 100 μg/ml concentrations in comparison to only LPS treated cells. The LDH activity in LPS + UA treated cells at 0.1 μM concentrations of UA was 1.25 ± 0.26, 1.43 ± 0.15 and 1.60 ± 0.18 per minute / mg of protein while at 1 μM concentrations of UA the activity was 1.19 ± 0.26, 1.23 ± 0.19 and 1.35 ± 0.19 per minute/mg of protein at 10, 50 and 100 μg/ml concentrations of LPS respectively (Fig. 2).

3.3. Mitochondrial membrane potential (MMP)

MMP was significantly ($p < 0.01$) decreased in the LPS treated N2A cells which was assessed by using fluorescent dye rhodamine123 (R123). The fluorescent intensity of R123 directly reflects the MMP as given in grabbed images and bar diagram (Fig. 3). The fluorescent intensity in control cells was 61.16 ± 5.07 whereas the intensity in LPS treated cells was 53.05 ± 4.08, 42.67 ± 1.65 and 39.12 ± 1.52 at 10, 50 and 100 μg/ml concentrations of LPS respectively. The fluorescent intensity in UA per se treated cells was 65.12 ± 5.01. Co-treatment of UA with the LPS showed significant ($p < 0.001$) increase in MMP at both 0.1 and 1 μM concentrations of UA with 50 and 100 μg/ml concentrations of LPS in comparison to only LPS treated cells. The fluorescent intensity in LPS + UA co-treated cells at 0.1 μM of UA was 55.29 ± 2.68, 60.82 ± 5.67 and 87.89 ± 3.82 while R123 intensity in cells treated with 1 μM of UA was 65.05 ± 5.10, 75.35 ± 6.67 and 95.52 ± 4.94 at 10, 50 and 100 μg/ml concentrations of LPS respectively.

3.4. ROS generation

ROS level was estimated by utilizing the cell-permeative dye DCF-DA. It is a fluorogenic dye that measures hydroxyl, peroxyl and different ROS levels inside the cell. After diffusion in to the cell, DCF-DA is deacetylated by cellular esterase to a nonfluorescent compound, which is later oxidized by ROS in to 2′, 7′- dichlorofluorescein (DCF). In control cells the basal ROS level was 399.40 ± 22.87 (a.u) which was significantly ($p < 0.001$) increased in cells treated with 10, 50 and 100 μg/ml concentrations of LPS and the fluorescence was 517.3067 ± 29.56, 522.015 ± 26.29 and 550.09 ± 27.37 respectively. The ROS level in UA per se treated cells was 410.89 ± 29.52 (a.u). Co treatment of UA with LPS offered significant attenuation of LPS induced augmented ROS level at both 0.1 μM and 1 μM concentration of UA. The fluorescence in cells treated with LPS + 0.1 μM of UA was 420.45 ± 22.7, 442.15 ± 25.15 and 429.22 ± 26.52 (a.u) while with 1 μM UA the fluorescence was 400.09 ± 22.51, 437.27 ± 25.38 and 376.977 ± 18.69 at 10, 50 and 100 μg/ml concentrations of LPS respectively (Fig. 4).

3.5. GSH level

GSH level was significantly ($p < 0.001$) diminished in the LPS treated N2A cells which was significantly ($p < 0.001$) restored with UA treatment. The GSH level in control cells was 99.18 ± 4.46 whereas in LPS treated cells the GSH level was 73.77 ± 1.17, 66.89 ± 1.46 and 47.65 ± 1.13 at 10, 50 and 100 μg/ml concentrations of LPS respectively. The GSH level in UA per se treated cells was 120.82 ± 3.37 which showed the significant augmentation in GSH level. The GSH level in LPS + UA treated cells at 0.1 μM of UA was 81.93 ± 0.91, 64.77 ± 2.06 and 65.17 ± 1.39. While the GSH levels at 1 μM of UA was 99.84 ± 0.93, 82.45 ± 1.58 and 73.19 ± 1.07 at 10, 50 and 100 μg/ml concentrations of LPS respectively (Fig. 5). The activity is expressed in μg/mg of protein.

3.6. mRNA level of pro-inflammatory cytokines

3.6.1. TNF-α level

LPS treatment to N2A cells caused significantly ($p < 0.05$) increased level of TNF-α. The level of TNF-α in control cells was 0.468 ± 0.014 which was increased to 0.554 ± 0.028, 0.634 ± 0.055 and 0.7114 ± 0.03 at 10, 50 and 100 μg/ml concentrations of LPS respectively. The TNF-α level in UA (1 μM) per se treated cells was 0.495 ± 0.029 which was not significantly different that control cells. Co-treatment of UA (1 μM) with LPS (100 μg/ml) did not offer protection against LPS induced increased TNF-α level and the value was 0.66 ± 0.03 (Fig. 6).

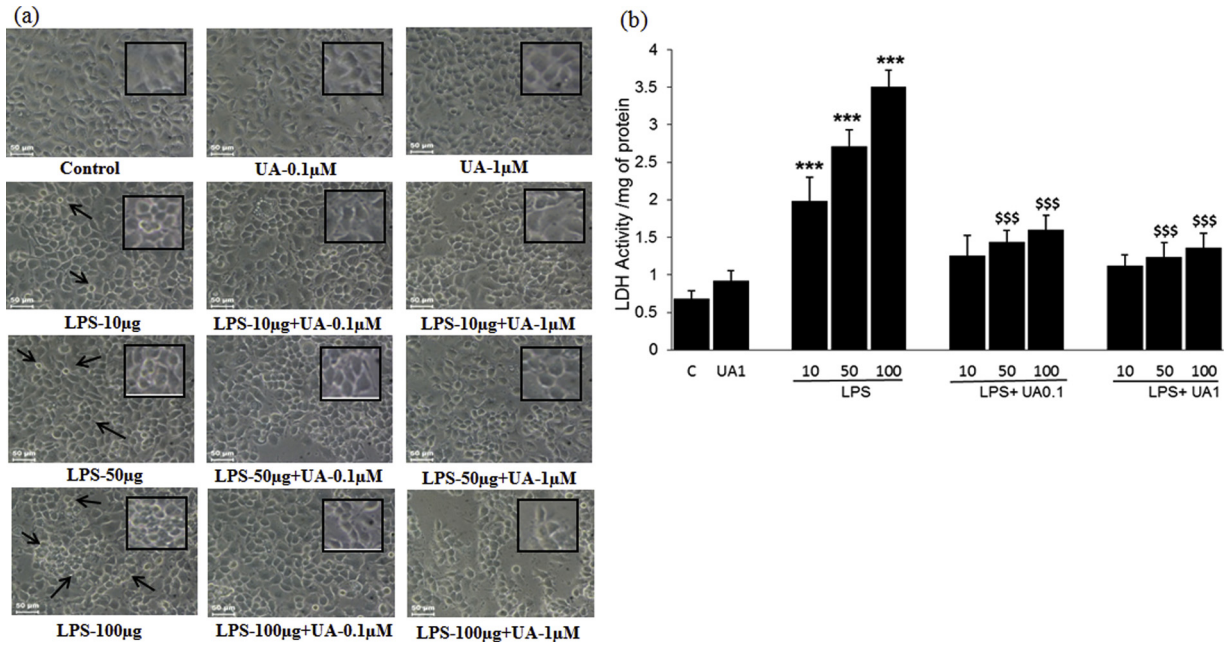

Fig. 2. (a) Bright field images & (b) Bar diagram illustrating the LDH activity in cells reflecting cytotoxicity in N2A cells after 24 h of treatment. Arrows are indicating the morphologically distorted cells and insets are showing the dying cells with high magnification. LPS caused a significant increase in cell toxicity. Ulmoside A (UA) showed significant protection against LPS induced adverse effects. Data are expressed as mean ± SEM, analyzed by one way ANOVA post hoc Newman Keuls multiple comparison test. ***p < 0.001 control vs. LPS and $$$p < 0.001 LPS vs. LPS + UA. Images were captured at 20X magnification.

3.6.2. IL-1β level

The IL-1β levels of in control cells was 0.521 ± 0.04 which was significantly ($p < 0.05$) increased to 0.624 ± 0.04 after LPS treatment at 100 μg/ml concentrations. The IL-1β level in per se UA (1 μM) treated cells was 0.485 ± 0.047 which was not significantly different than level of control cells. Co-treatment of UA (1 μM) with LPS (100 μg/ml) did not offer protection against LPS induced increased IL-1β level and the value was 0.58 ± 0.05 (Fig. 6).

3.7. Protein level of pro-inflammatory cytokines

The LPS treatment to N2A cells caused significant increase in level

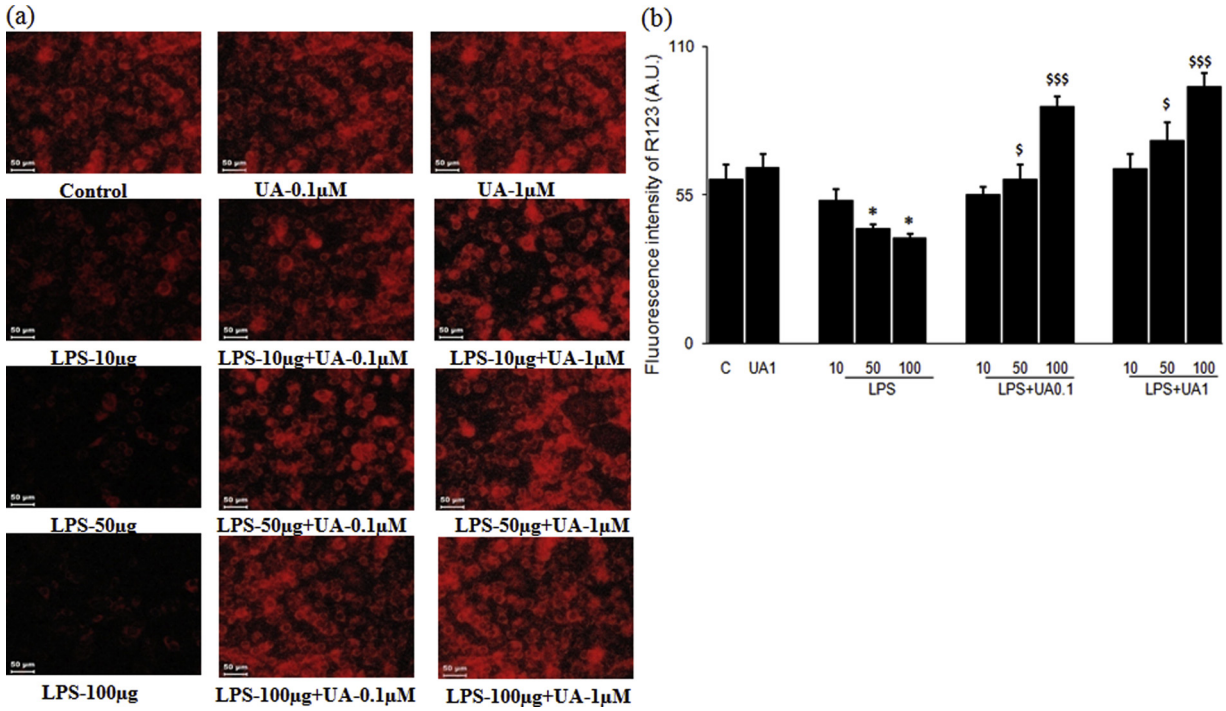

Fig. 3. (a) Images represents the altered mitochondrial membrane potential (Rhodamine 123 fluorescence) (b) Bar diagram illustrating the altered mitochondrial membrane potential in N2A cells after 24 h of treatment with different concentration of LPS & Ulmoside A (UA). Data are expressed as mean ± SEM, analyzed by one way ANOVA post hoc Newman Keuls multiple comparison test. *p < 0.1 control vs. LPS and $p < 0.05, $$$p < 0.001 LPS vs. LPS + UA. Images were captured at 20X magnification.

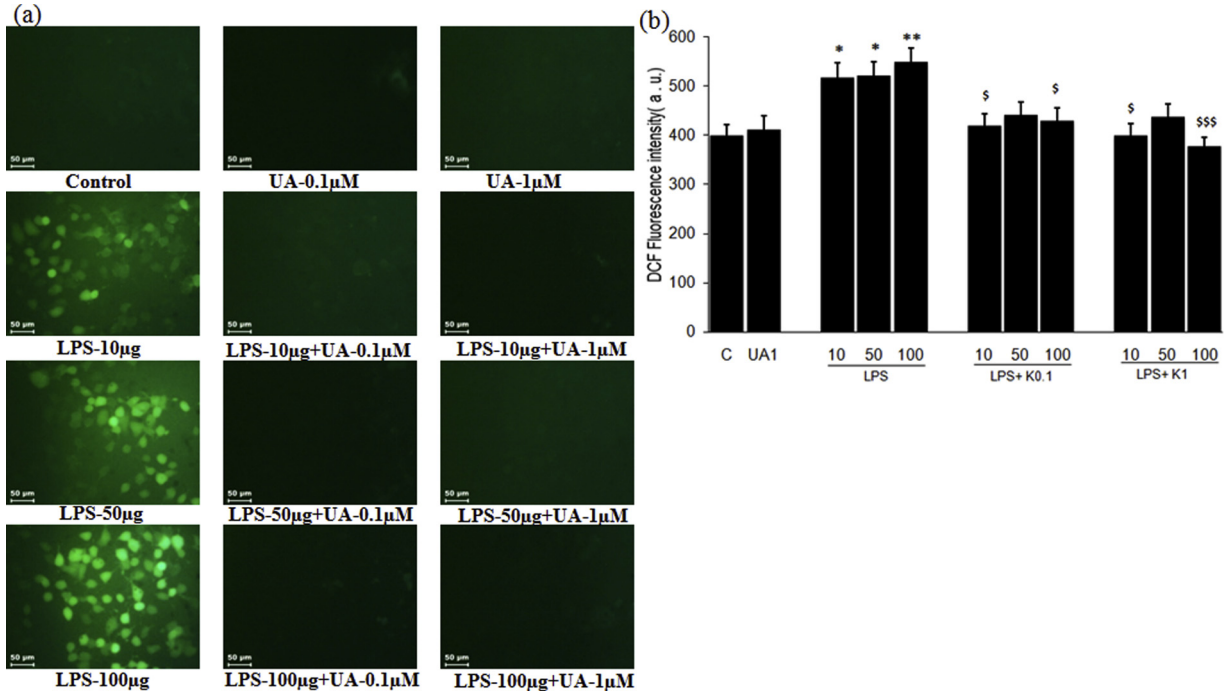

Fig. 4. (a) Images indicate the DCF fluorescence reflecting the reactive oxygen species (ROS) generation (b) Bar diagram showed the quantification of DCF fluorescence in N2A cells after 24 h of treatment. LPS treatment exhibited the increased level of ROS in N2A cells which was significantly restored with co-treatment of Ulmoside A (UA). Data are expressed as mean ± SEM, analyzed by one way ANOVA post hoc Newman Keuls multiple comparison test. *p < 0.05, **p < 0.01 control vs. LPS and $p < 0.05, $$$p < 0.001 LPS vs. LPS + UA. Images were captured at 20X magnification.

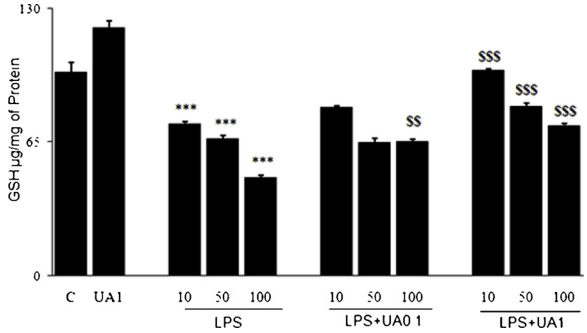

Fig. 5. Bar diagram showed the level of GSH in N2A cells after 24 h of treatment. LPS administration exhibited the decreased level of GSH in N2A cells which was significantly restored with co-treatment of Ulmoside A (UA). Data are expressed as mean ± SEM, analyzed by one way ANOVA post hoc Newman Keuls multiple comparison test. ***p < 0.001 control vs. LPS and $$p < 0.01 & $$$p < 0.001 LPS vs. LPS + UA.

of TNF-α and IL-1β protein which were not significantly altered with UA treatment (Fig. 7). In control cells the TNF-α level was 0.92 ± 0.1 while the level in LPS treated cells was 1.02 ± 0.1. Co treatment of UA did not offer any significant alteration in LPS induced augmented TNF α level. Similarly in control cells the IL-1β level was 0.69 ± 0.02 which was increased to 0.83 ± 0.1. However, co treatment of UA did not offer any protection against LPS induced increased IL-1β level.

3.8. Assessment of apoptosis related marker proteins-

3.8.1. Cytochrome c translocation

The LPS treatment caused significant ($p < 0.01$) translocation of cytochrome-c in cytosol from mitochondria as detected by western blot in mitochondrial and cytosolic fraction of N2A cells. Co-treatment of UA (1 μM) with LPS significantly ($p < 0.05$) restored the cytochrome-c level in the mitochondrial fraction of cells and significantly ($p < 0.01$) decreased the translocation of cytocrome-c in cytosol (Fig. 8).

3.8.2. Expression of Bax, Bcl-2 and cleaved caspase-3

The LPS treatment to N2A cells caused significantly ($p < 0.01$) increased level of cleaved caspase-3 and pro-apoptotic Bax proteins which was significantly ($p < 0.01$) reduced on co-treatment with UA (1 μM). Concomitantly LPS treatment caused significant ($p < 0.001$) decrease in expression of anti-apoptotic Bcl-2 protein which was significantly recovered on co-treatment with UA (1 μM) (Fig. 9).

3.8.3. Expression of iNOS and cleaved PARP

The LPS treatment to N2A cells caused increased expression of iNOS level which was not significantly affected with co-treatment of UA. LPS treatment caused significantly ($p < 0.05$) increased level of cleaved PARP which was significantly ($p < 0.01$) reduced with co-treatment of UA (1 μM) with LPS (Fig. 10).

3.8.4. Assessment of phosphatidylserine (PS) externalization in LPS treated neuronal cells

PS externalization is the early marker of apoptosis estimated by Annexin V-FITC staining directly reflecting the number of cells undergoing early and late apoptosis. The LPS treatment led to significant ($p < 0.001$) augmentation in Annexin V-FITC positive cells in compare to control cells (Fig. 11). The percentage of Annexin V-FITC positive cells showing early apoptosis was 10.6 percent at 100 μg/ml concentration of LPS in comparison with control cells. In control cells the percentage of early and late apoptotic cells was 2.08 and 0.73 percent respectively. Co-treatment of UA exhibited significant ($p < 0.001$) protection in early apoptotic cells and the levels were decreased to 3.2 and 3.3 percent at UA0.1 μM and UA1 μM concentration respectively. Cells which are undergoing late apoptotic or necrotic stage will be stained with both Annexin V-FITC and PI dye. Late apoptotic cells were also observed after LPS treatment and the percentage of late apoptotic cells was 76.78 percent which was significantly ($p < 0.001$) different in comparison to control cells. Co-treatment of UA with LPS offered

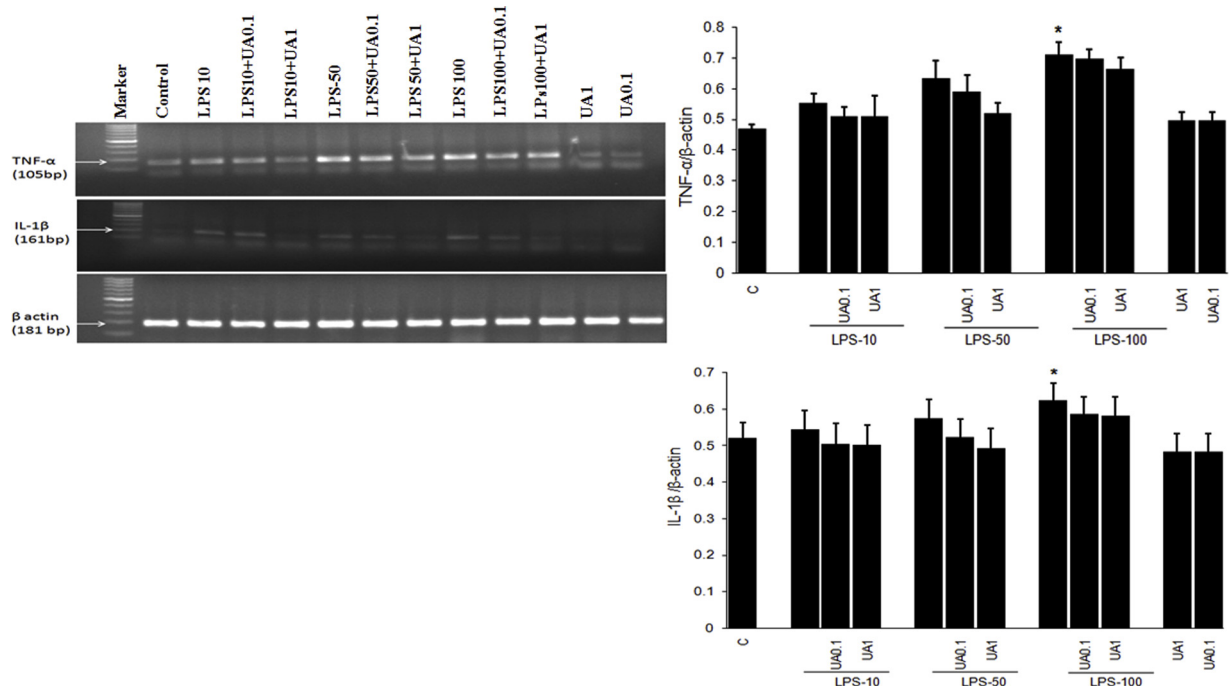

Fig. 6. Images and bar diagram for mRNA level of inflammatory cytokines (TNF-α & IL-1β) assessed by reverse transcriptase PCR in N2A cells after 24 h treatment of LPS and Ulmoside A (UA). Cytokines expression were increased at highest concentrations of LPS but no significant alteration was observed with UA treatment though the levels were reduced. Data are expressed as mean ± SEM, analyzed by one way ANOVA post hoc Newman Keuls multiple comparison test. *p < 0.05 control vs. LPS.

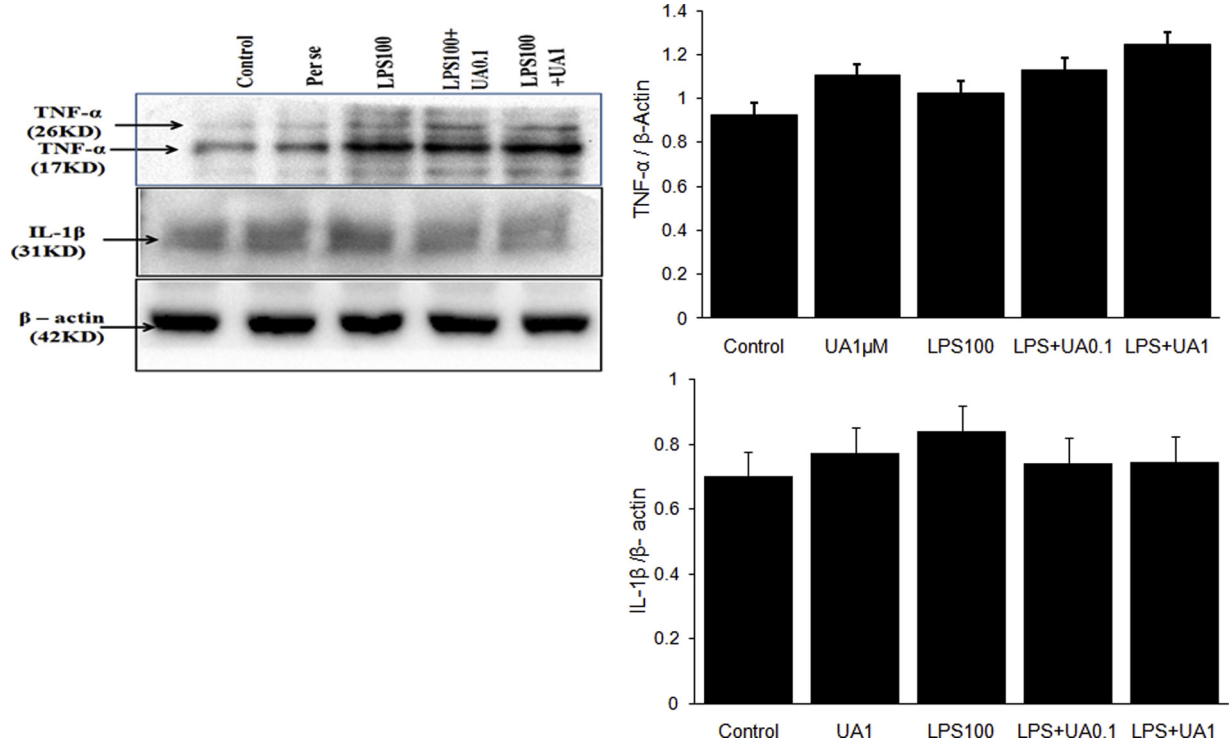

Fig. 7. Bar diagram and images of blots for protein levels of inflammatory cytokines (TNF-α & IL-1β) assessed by western blotting in N2A cells after 24 h treatment of LPS and Ulmoside A (UA). LPS caused the considerable increase in both cytokines however, no significant alteration was observed with UA treatment though the levels were reduced. Data are expressed as mean ± SEM, analyzed by one way ANOVA post hoc Newman Keuls multiple comparison test.

significant ($p < 0.01$) protection in the LPS induced loss of cell membrane integrity, and the number of Annexin V-FITC stained cells was lessened to 1.25 and 1.21% at 0.1μM and 1 μM concentrations of UA respectively.

3.9. DNA fragmentation

Single cell gel electrophoresis assay was performed to evaluate the DNA fragmentation in control, LPS treated, UA treated, z-VAD treated, melatonin treated, LPS + UA treated, LPS + melatonin and LPS + z-

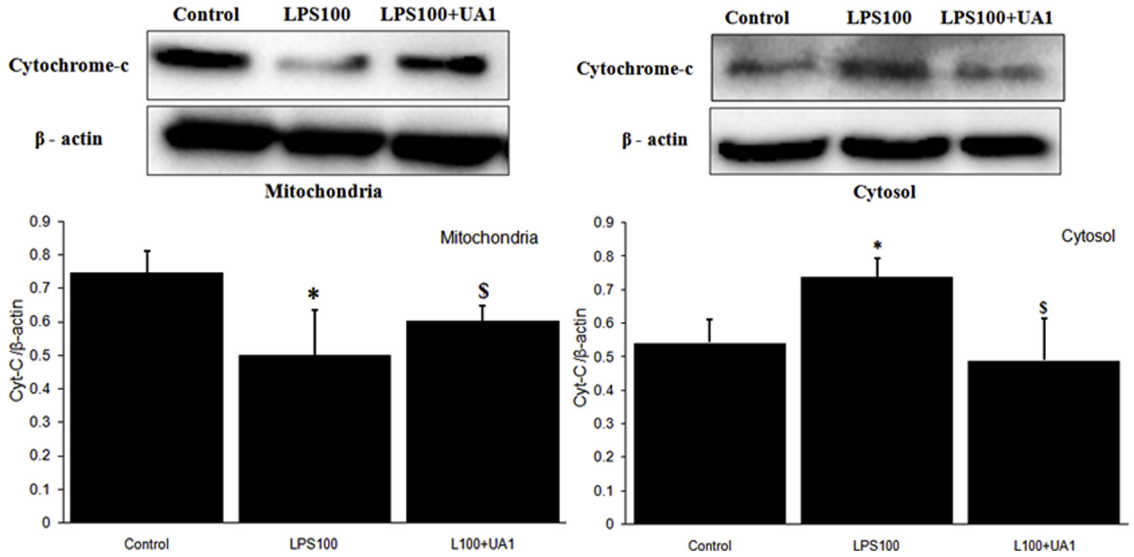

Fig. 8. Images and bar diagram indicating the level of cytochrome c in mitochondria and cytosol fraction of N2A cells after 24 h treatment of LPS and Ulmoside A (UA). LPS treatment caused significant translocation of cytochrome c in cytosol from the mitochondria which was inhibited with UA treatment. Data are expressed as mean ± SEM and analyzed by ANOVA post hoc Newman-Keuls multiple comparison test. *p < 0.01 control vs. LPS treated cells. $p < 0.01 LPS vs. LPS + UA.

VAD-treated N2A cells (Fig. 12). Comet parameter olive tail moment (OTM) was analyzed by CASP software. OTM is defined as the product of the TL and the fraction of total DNA in the tail. LPS treatment caused significant ($p < 0.001$) increase in OTM in comparison to control cells. LPS treatment to N2A cells caused significantly ($p < 0.001$) increased OTM in concentration dependent manner. The fluorescent intensity for OTM in control N2A cells was 7.32 ± 1.13 whereas the OTM was 29.09 ± 1.85, 38.14 ± 2.65 and 62.08 ± 3.28 at 10, 50 and 100 μg/ml concentrations of LPS respectively. Per se treatment of UA (1 μM) did not alter the comet parameters in comparison to control cells. The values of OTM in only UA treated N2A cells was 7.61 ± 1.10. Co-treatment of LPS with UA offer significant ($p < 0.001$) protection against LPS induced DNA fragmentation in N2A cells. The OTM of the pretreatment of z-VAD and melatonin to N2A cells also prevent the LPS induced DNA damage.

4. Discussion

Findings of the present study indicated the antioxidative and anti-apototic activities of isolated flavonoid Ulmoside A. LPS treatment to

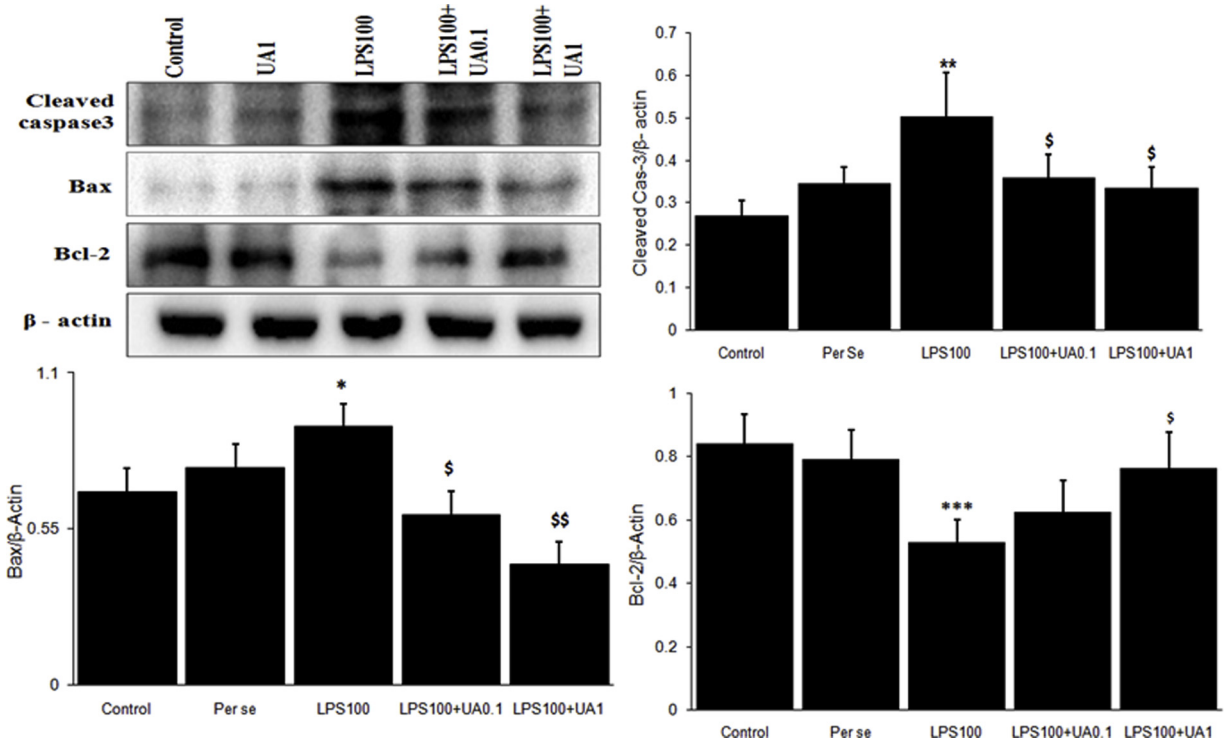

Fig. 9. Pictorial and graphical representation for level of cleaved caspase 3, Bax and Bcl-2 in N2A cells after 24 h of treatment of LPS and Ulmoside A (UA). LPS treatment caused significantly increased level of cleaved caspase-3 and Bax while the level of Bcl-2 was significantly inhibited. UA caused significant attenuation against LPS induced alterations. Data are expressed as mean ± SEM and analyzed by ANOVA post hoc Newman-Keuls multiple comparison test. *p < 0.05, **p < 0.01 control vs. LPS. $p < 0.01 LPS vs. LPS + UA.

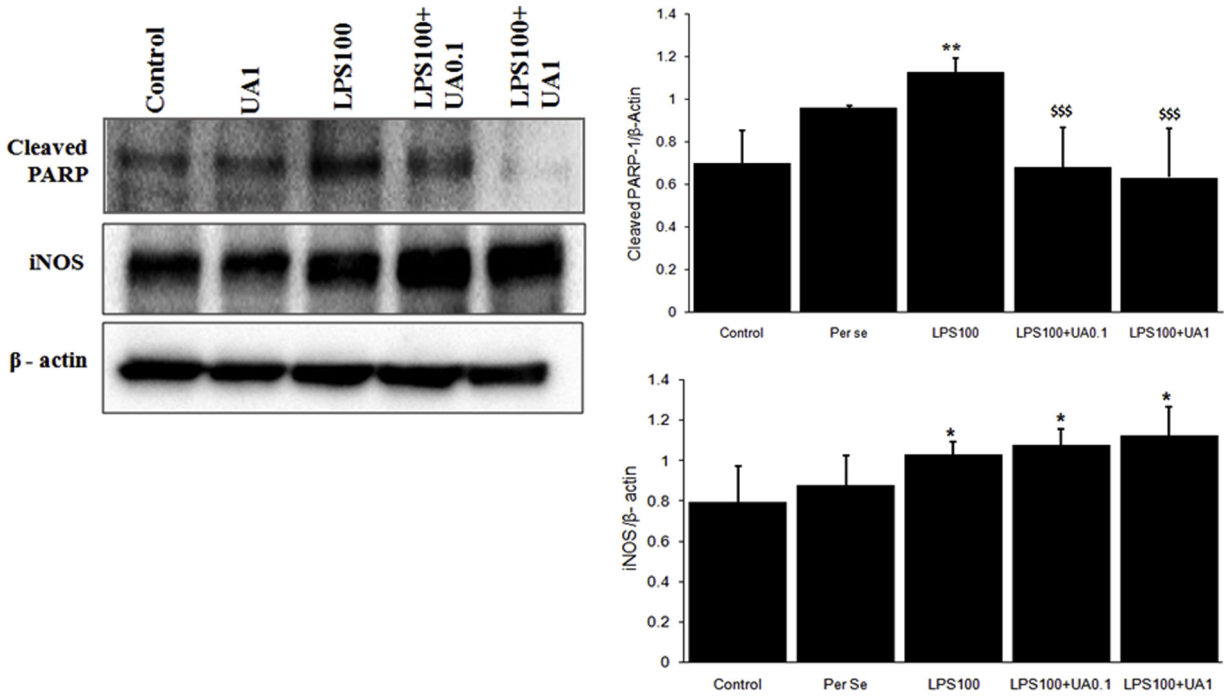

Fig. 10. Images & bar diagram represent the protein level of cleaved PARP and iNOS level in N2A cells after 24 h treatment of LPS and LPS + Ulmoside A (UA). LPS treatment caused significant increase in level of cleaved PARP-1. iNOS level was significantly increased with LPS treatments. Data are expressed as mean ± SEM and analyzed by ANOVA post hoc Newman-Keuls multiple comparison test. *p < 0.05, **p < 0.01 control vs. LPS $$$p < 0.01 LPS vs. LPS + UA.

the neuronal cells caused significantly decreased cell viability and distorted cellular morphology. Co-treatment of UA exhibited the restored cellular viability, cytotoxicity and cellular morphology. LPS induced decreased mitochondrial dehydrogenase activity was collated with decreased mitochondrial membrane potential reflecting the LPS induced impaired mitochondrial activity. The LPS induced decreased mitochondrial membrane potential was significantly restored with UA treatment. Previously also flavonoid induced protection against oxidative stress and apoptosis is reported. Pinocembrin (5, 7-dihydroxyflavanone), a natural flavonoid attenuates the oxidative perturbations, inflammation and apoptosis in a rat model of global cerebral ischemia reperfusion (Saad et al., 2015). Pinocembrin could also protect the neuroblastoma SH-SY5Y cells from Aβ25–35 induced neurotoxicity through activation of Nrf2/HO-1 pathways and inhibition of mitochondria-dependent apoptosis (Wang et al., 2016). Santos et al (1998) compared the eight structurally related natural flavonoids and reported the order of potency of these flavonoids in inhibition of lipid peroxidation, mitochondrial membrane permeability transition pore

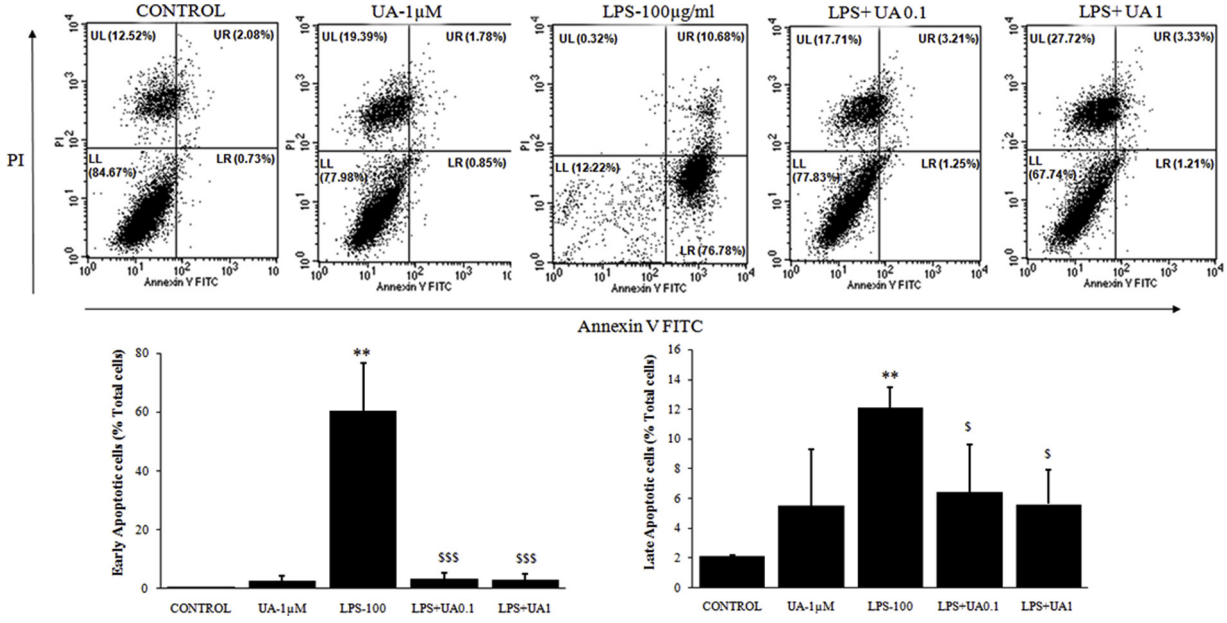

Fig. 11. Representative image of flow cytometry in LPS and/or LPS + Ulmoside A (UA) treated N2A cells. Bar diagram of early and late apoptotic cells in control and treated sets. LPS caused significant increase in early and late apoptosis in cells which was significantly attenuated with UA treatment. Data are expressed as mean ± SEM and analyzed by ANOVA post hoc Newman-Keuls multiple comparison test. **p < 0.01 control vs. LPS. $p < 0.05, $$p < 0.01, $$$p < 0.001 LPS vs. LPS + UA.

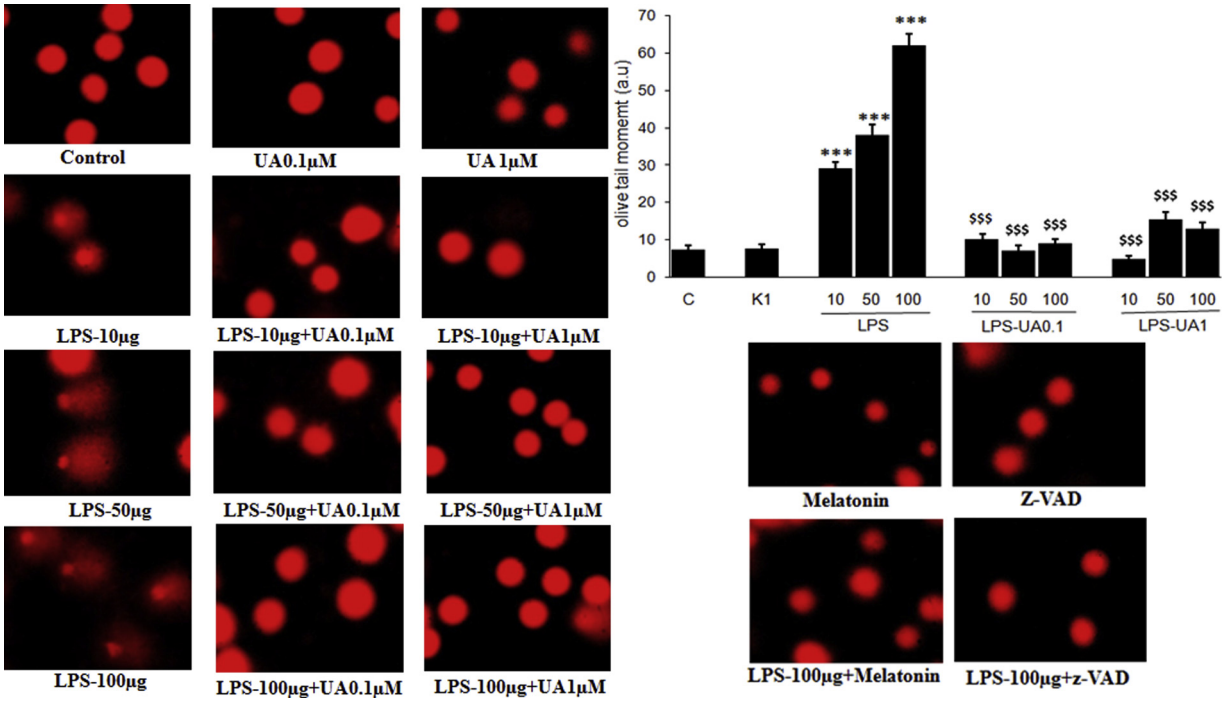

Fig. 12. Comet pictures showing the effect of LPS and LPS + Ulmoside A (UA) in N2A cells after 24 h treatment. Olive tail showing the LPS induced DNA damage. Cells were also treated with melatonin (1 mM) and z-VAD (20μM). No significant DNA fragmentation was observed in N2A cells with treatment of melatonin and z-VAD. LPS (100 μg) and melatonin/z-VAD treated cells exhibited the protection against LPS induced DNA fragmentation. Data are expressed as mean ± SEM and analyzed by ANOVA post hoc Newman-Keuls multiple comparison test. ***$p < 0.01$ control vs. LPS. \$\$\$$p < 0.01$ LPS vs. LPS + UA.

formation and oxidative stress. Nitric oxide/cGMP pathway mediated anti hypertensive activity of extract of U. wallichiana has also been reported in rats through modulating rennin-angiotensin-aldosterone axis (Syed et al., 2016). It could also offer cardioprotective activity in rats against isoprenaline cardiac hypertrophy involving nitric oxide and inflammatory pathways (Syed et al., 2016). With this view we have estimated the level of reactive oxygen species (ROS) and level of GSH in control and treated N2A cells, considered as parameter of oxidative stress. LPS treatment caused significantly increased level of ROS and depleted level of GSH which was significantly attenuated with UA treatment. Higher concentration of UA offered better attenuation against LPS induced depleted GSH level in comparison to lower concentration of UA suggesting dose dependent effects. Another flavonoid Silymarin exhibited the potential antidepressant-like activity in mice through modulating corticosterone and oxidative stress response in cerebral cortex and hippocampus (Thakare and Dhakane, 2016). Flovanoid pinocembrin induced cellular protection also associated with the reduced level of ROS, nitric oxide and augmented GSH level. Study by Guang and Du (2006) reported that pinocembrin could improve the cognitive impairments in rats by protecting brain mitochondrion structure and function. Another study by Sharma et al (2013) reported that flavonoid quercetin offered neuroprotection against aluminium induced cognitive impairments, cholinergic dysfunction, and associated oxidative damage in rats. Flavonol morin induced attenuation against chronic constriction injury has also been reported which involve the inhibition of oxidative stress induced PARP over activation and neuroinflammation (Komirishetty et al., 2016). To assess the effect of UA on inflammatory parameters we have investigated the level of proinflammatory cytokines. LPS treatment to N2A cells exhibited the increased level of TNF-α and IL-1β. However, co treatment of UA did not offer significant inhibition against LPS induced adverse effects suggesting that UA did not offer anti-inflammatory properties in LPS treated neuronal cells. Since significant mitochondria impairment was observed in LPS treated neuronal cells further we would like to investigate the effect of UA on LPS induced apoptotic signaling. Earlier we have reported that LPS treatment caused significant translocation of cytochrome-c in cytosol from mitochondria (Singh et al., 2010). Such translocated cytochrome-c may initiate the intrinsic apoptotic pathway therefore further investigation was done in this direction. LPS treatment to N2A cells exhibited the significant cytochrome-c translocation in cytosol from mitochondria which was collated with inhibited Bcl-2 and augmented Bax levels. In addition to altered level of Bax and Bcl-2, significantly increased level of cleaved caspase-3 was also observed in LPS treated N2A cells. LPS induced induction in such pro-apoptotic factors were significantly inhibited with UA treatment. In this context reports available showed the flavonoids induced antiapoptotic effects. A novel flavonoid from the stem-bark of U. Wallichiana Planchon stimulates the osteoblast function and inhibits osteoclast and adipocyte differentiation through apoptotic pathways (Swarnkar et al., 2011). Chen et al (2017) reported that morin, a flavonol exhibits the potent anti-oxidative and anti-apoptotic activity. Morin could elevate the antioxidant enzyme (SOD, GSH, GPx) levels and down regulate the Bax and caspase-3 in focal cerebral ischemic rats. Another report suggested that water soluble morin-5′-sulfonic acid sodium salt inhibits the mercuric chloride induced altered level of Bax, Bcl-2 and caspase-3 through its effective chelation action (Venkatesan and Sadiq, 2017). Another flavonoid isoquercetin also effectively alleviated the hippocampus neuronal apoptosis by regulating cyclic AMP responsive element-binding protein (CREB), Bax, Bcl-2, and caspase-3 (Wang et al., 2017). In addition to altered level of proapoptotic and antiapoptotic factors we have also observed the LPS induced significantly increased level of inducible nitric oxide synthase (iNOS) but UA did not offer any inhibition against such augmented iNOS levels, suggesting the critical interference of UA in oxidative stress mediated neuronal death. Besides alteration in apoptotic factors and oxidative stress, LPS induced significant DNA fragmentation was observed which is in agreement to previous findings reported by us and others (Chen et al., 2007; Dholakiya and Benzeroual, 2011; Verma et al., 2018b). LPS induced DNA fragmentation was significantly inhibited with UA treatment. To validate that UA mediated inhibition of DNA fragmentation was interceding through its

interference in oxidative and apoptotic pathways, the cells were also co treated with melatonoin (an antioxidant) and z-VAD (broad spectrum caspase inhibitor). Findings indicated that the observed inhibitory effects of UA on DNA fragmentation involve oxidative and apoptotic pathways as both melatonin and z-VAD exhibited the similar protection against LPS induced DNA fragmentation as observed with UA treatment. In agreement to our findings other reports have also suggested the flavonoids induced improvement in mitochondrial function (Luan et al., 2018), mutagenic effects (Abo-Zeid et al., 2018), cytotoxicity and apoptosis (Bijak et al., 2017; Kim et al., 2017; Velagapudi et al., 2018). Flavonol quercetin also showed the protection to dopaminergic neurons against endoplasmic reticulum stress and apoptosis (Park and Chun, 2016; Sharma et al., 2016). In conclusion findings suggested that UA treatment offered significant neuronal protection against LPS induced cytotoxicity, mitochondrial impairment, depleted GSH level, ROS generation, cytochrome-c translocation, PARP cleavage, Bcl2 depletion, augmented level of Bax, cleavage of caspase-3 and DNA fragmentation. Observation suggested that UA induced protection primarily offered by acting on oxidative stress and apoptotic pathways suggesting anti-oxidative and anti-apoptotic activity of UA.

Conflict of interest

Authors have no conflict of interest.

Acknowledgement

The funding support was received from SERB, India with grant number EMR/2015/001282.

References

Abo-Zeid, M.A.M., Abdel-Samie, N.S., Farghaly, A.A., Hassan, E.M., 2018. Flavonoid fraction of Cajanuscajan prohibited the mutagenic properties of cyclophosphamide in mice in vivo. Mutat. Res. 826 (Febuary), 1–5.

Agati, G., Azzarello, E., Pollastri, S., Tattini, M., 2012. Flavonoids as antioxidants in plants: location and functional significance. Plant Sci. 196 (November), 67–76.

Apetz, N., Munch, G., Govindaraghavan, S., Gyengesi, E., 2014. Natural compounds and plant extracts as therapeutics against chronic inflammation in Alzheimer's disease–a translational perspective. CNS Neurol. Disord. Drug Targets 13 (7), 1175–1191.

Bensouici, C., Kabouche, A., Karioti, A., Öztürk, M., Duru, M.E., Bilia, A.R., Kabouche, Z., 2016. Compounds from Sedum caeruleum with antioxidant, anticholinesterase, and antibacterial activities. Pharm. Biol. 54 (1), 174–179.

Bijak, M., Synowiec, E., Sitarek, P., Sliwiński, T., Saluk-Bijak, J., 2017. Evaluation of the cytotoxicity and genotoxicity of flavonolignans in different cellular models. Nutrients 9 (December (12)), pii: E1356.

Biswas, J., Goswami, P., Gupta, S., Joshi, N., Nath, C., Singh, S., 2016. Streptozotocin induced neurotoxicity involves Alzheimer's related pathological markers: a study on N2A cells. Mol. Neurobiol. 53 (July (5)), 2794–2806.

Bose, B., Choudhury, H., Tandon, P., Kumaria, S., 2017. Studies on secondary metabolite profiling, anti-inflammatory potential, in vitro photoprotective and skin-aging related enzyme inhibitory activities of Malaxisacuminata, a threatened orchid of nutraceutical importance. J. Photochem. Photobiol. B 173 (August), 686–695.

Brunetti, C., Di Ferdinando, M., Fini, A., Pollastri, S., Tattini, M., 2013. Flavonoids as antioxidants and developmental regulators: relative significance in plants and humans. Int. J. Mol. Sci. 14 (February (2)), 3540–3555.

Chen, P.S., Wang, C.C., Bortner, C.D., Peng, G.S., Wu, X., Pang, H., Lu, R.B., Gean, P.W., Chuang, D.M., Hong, J.S., 2007. Valproic acid and other histone deacetylase inhibitors induce microglial apoptosis and attenuate lipopolysaccharide-induced dopaminergic neurotoxicity. Neuroscience 149 (October (1)), 203–212 Epub 2007 Jul 28.

Chen, S., Yuan, J., Yao, S., Jin, Y., Chen, G., Tian, W., Xi, J., Xu, Z., Weng, D., Chen, J., 2015. Lipopolysaccharides may aggravate apoptosis through accumulation of autophagosomes in alveolar macrophages of human silicosis. Autophagy 11 (12), 2346–2357.

Chen, Y., Li, Y., Xu, H., Li, G., Ma, Y., Pang, Y.J., 2017. Morin mitigates oxidative stress, apoptosis and inflammation in cerebral ischemic rats. Afr. J. Tradit. Complement. Altern. Med. 14 (January (2)), 348–355.

Davinelli, S., Bertoglio, J.C., Polimeni, A., Scapagnini, G., 2018. Cytoprotective polyphenols against chronological skin aging and cutaneous photodamage. Curr. Pharm. Des. 24 (2), 99–105.

Dholakiya, S.L., Benzeroual, K.E., 2011. Protective effect of diosmin on LPS-induced apoptosis in PC12 cells and inhibition of TNF-α expression. Toxicol. In Vitro 25 (August (5)), 1039–1044. https://doi.org/10.1016/j.tiv.2011.04.003. Epub 2011 Apr 6.

Dilshara, M.G., Lee, K.T., Kim, H.J., Lee, H.J., Choi, Y.H., Lee, C.M., Kim, L.K., Kim, G.Y., 2014. Anti-inflammatory mechanism of α-viniferin regulates lipopolysaccharide-induced release of proinflammatory mediators in BV2 microglial cells. Cell. Immunol. 290 (July (1)), 21–29.

Fernandes, V., Sharma, D., Kalia, K., Tiwari, V., 2018. Neuroprotective effects of silibinin: an in silico and in vitro study. Int. J. Neurosci. 15 (March), 1–11.

Fernández-Moriano, C., Gómez-Serranillos, M.P., Crespo, A., 2016. Antioxidant potential of lichen species and their secondary metabolites. A systematic review. Pharm. Biol. 54 (1), 1–17.

Giorgio, M., Migliaccio, E., Orsini, F., Paolucci, D., Moroni, M., Contursi, C., 2005. Electron transfer between cytochrome-c and p66shc generates reactive oxygen species that trigger mitochondrial apoptosis. Cell 122, 221–233.

Guang, H.M., Du, G.H., 2006. Protections of pinocembrin on brain mitochondria contribute to cognitive improvement in chronic cerebral hypoperfused rats. Eur. J. Pharmacol. 542 (August (1-3)), 77–83 Epub 2006 May 12.

Gupta, S., Verma, D.K., Biswas, J., Siva Rama Raju, K., Joshi, N., Wahajuddin, Singh S., 2014. The metabolic enhancer piracetam attenuates mitochondrion-specific endonuclease g translocation and oxidative DNA fragmentation. Free Radic. Biol. Med. 73, 278–290.

Hail, N., JrLotan, R., 2000. Mitochondrial permeability transition is a central coordinating event in N-(4-hydroxyphenyl) retinamide-induced apoptosis. Cancer Epidemiol. Biomarkers Prev. 9, 1293–1301.

Houghton, P.J., Howes, M.J., 2005. Natural products and derivatives affecting neurotransmission relevant to Alzheimer's and Parkinson's disease. Neurosignals 14 (1-2), 6–22.

Javed, H., Khan, M.M., Ahmad, A., Vaibhav, K., Ahmad, M.E., Khan, A., Ashafaq, M., Islam, F., Siddiqui, M.S., Safhi, M.M., Islam, F., 2012. Rutin prevents cognitive impairments by ameliorating oxidative stress and neuroinflammation in rat model of sporadic dementia of Alzheimer type. Neuroscience 17 (210), 340–352.

Khan, M.P., Mishra, J.S., Sharan, K., Yadav, M., Singh, A.K., Srivastava, A., Kumar, S., Bhaduaria, S., Maurya, R., Sanyal, S., Chattopadhyay, N., 2013. A novel flavonoid C-glucoside from Ulmus wallichiana preserves bone mineral density, microarchitecture and biomechanical properties in the presence of glucocorticoid by promoting osteoblast survival: a comparative study with human parathyroid hormone. Phytomedicine 20 (November (14)), 1256–1266.

Kim, B.W., Koppula, S., Hong, S.S., Jeon, S.B., Kwon, J.H., Hwang, B.Y., Park, E.J., Choi, D.K., 2013. Regulation of microglia activity by glaucocalyxin-A: attenuation of lipopolysaccharide-stimulated neuroinflammation through NF-κB and p38 MAPK signaling pathways. PLoS One 8 (2), e55792.

Kim, B.W., Koppula, S., Park, S.Y., Kim, Y.S., Park, P.J., Lim, J.H., Kim, I.S., Choi, D.K., 2015a. Attenuation of neuroinflammatory responses and behavioral deficits by Ligusticumofficinale (Makino) Kitag in stimulated microglia and MPTP-induced mouse model of Parkinson's disease. J. Ethnopharmacol. 22 (April (164)), 388–397.

Kim, M.J., Park, M., Kim, D.W., Shin, M.J., Son, O., Jo, H.S., Yeo, H.J., Cho, S.B., Park, J.H., Lee, C.H., Kim, D.S., Kwon, O.S., Kim, J., Han, K.H., Park, J., Eum, W.S., Choi, S.Y., 2015b. Transduced PEP-1-PON1 proteins regulate microglial activation and dopaminergic neuronal death in a Parkinson's disease model. Biomaterials 64 (September), 45–56.

Kim, S., Chin, Y.W., Cho, J., 2017. Protection of cultured cortical neurons by Luteolin against oxidative damage through inhibition of apoptosis and induction of heme oxygenase-1. Biol. Pharm. Bull. 40 (3), 256–265.

Komirishetty, P., Areti, A., Sistla, R., Kumar, A., 2016. Morin mitigates chronic constriction injury (CCI)-Induced peripheral neuropathy by inhibiting oxidative stress induced PARP over-activation and neuroinflammation. Neurochem. Res. 41 (August (8)), 2029–2042.

Kuwabara, T., Imajoh-Ohmi, S., 2004. LPS-induced apoptosis is dependent upon mitochondrial dysfunction. Apoptosis 9, 467–474.

Lee, S.H., Lee, J.H., Oh, E.Y., Kim, G.Y., Choi, B.T., Kim, C., Choi, Y.H., 2013. Ethanol extract of Cnidiumofficinale exhibits anti-inflammatory effects in BV2 microglial cells by suppressing NF-κB nuclear translocation and the activation of the PI3K/Akt signaling pathway. Int. J. Mol. Med. 32 (October (4)), 876–882.

Leuner, K., Kurz, C., Guidetti, G., Orgogozo, J.M., Muller, W.E., 2010. Improved mitochondrial function in brain aging and Alzheimer disease – the new mechanism of action of the old metabolic enhancer piracetam. Front. Neurosci. 7 (44).

Lowry, O.H., Rosebrough, N.J., Farr, A.I., Randall, R.J., 1951. Protein measurement with the Folin phenol reagent. J. Biol. Chem. 193, 265–275.

Luan, G., Wang, Y., Wang, Z., Zhou, W., Hu, N., Li, G., Wang, H., 2018. Flavonoid glycosides from fenugreek seeds regulate glycolipid metabolism by improving mitochondrial function in 3T3-L1 adipocytes in vitro. J. Agric. Food Chem. 66 (March (12)), 3169–3178.

Maurya, R., Singh, G., Yadav, P.P., 2008. Antiosteoporotic agents from natural sources. In: Rahman, A.U. (Ed.), Studies in Natural Product Chemistry, Bioactive Natural Products. Elsevier, New York, NY, pp. 517–548.

Moreira, P.I., Carvalho, C., Zhu, X., Smith, M.A., Perry, G., 2010. Mitochondrial dysfunction is a trigger of Alzheimer's disease pathophysiology. Biochim. Biophys. Acta 1802, 2–10.

Ning, Q., Liu, Z., Wang, X., Zhang, R., Zhang, J., Yang, M., Sun, H., Han, F., Zhao, W., Zhang, X., 2017. Neurodegenerative changes and neuroapoptosis induced by systemic lipopolysaccharide administration are reversed by dexmedetomidine treatment in mice. Neurol. Res. 39 (April (4)), 357–366.

Park, E., Chun, H.S., 2016. Protective effects of quercetin on dieldrin-induced endoplasmic reticulum stress and apoptosis in dopaminergic neuronal cells. Neuroreport. 27 (October (15)), 1140–1146.

Plummer, S., Van den Heuvel, C., Thornton, E., Corrigan, F., Cappai, R., 2016. The neuroprotective properties of the amyloid precursor protein following traumatic brain injury. Aging Dis. 7 (March (2)), 163–179.

Rawat, P., Kumar, M., Sharan, K., Chattopadhyay, N., Maurya, R., 2009. Ulmosides A and

B: flavonoid 6-C-glycosides from *Ulmus wallichiana*, stimulating osteoblast differentiation assessed by alkaline phosphatase. Bioorg. Med. Chem. Lett. 4684–4687.
Reed, J.C., Green, D.R., 1998. Mitochondria and apoptosis. Science 281, 1309–1312.
Ryu, J.K., Nagai, A.Kim, Lee, J., McLarnon, M.C., Kim, J.G., 2003. S.U. Microglial activation and cell death induced by the mitochondrial toxin3-nitropropionic acid, in vitro and in vivo studies. Neurobiol. Dis. 12, 121–132.
Saad, M.A., Abdel Salam, R.M., Kenawy, S.A., Attia, A.S., 2015. Pinocembrin attenuates hippocampal inflammation, oxidative perturbations and apoptosis in a rat model of global cerebral ischemia reperfusion. Pharmacol. Rep. 67 (February (1)), 115–122.
Santos, A.C., Uyemura, S.A., Lopes, J.L., Bazon, J.N., Mingatto, F.E., Curti, C., 1998. Effect of naturally occurring flavonoids on lipid peroxidation and membrane permeability transition in mitochondria. Free Radic. Biol. Med. 24 (June (9)), 1455–1461.
Sarkar, F.H., Rahman, K.M., Li, Y., 2003. Bak translocation to mitochondria is an important event in inducing apoptotic cell death by indole-3-carbinol (I3C) treatment of breast cancer cells. J. Nutr. 133, 2434–2439.
Scotti, L., Scotti, M.T., 2015. Computer aided drug design studies in the discovery of secondary metabolites targeted against age-related neurodegenerative diseases. Curr. Top. Med. Chem. 15 (21), 2239–2252.
Sharan, K., Swarnkar, G., Siddiqui, J.A., Kumar, A., Rawat, P., Kumar, M., Nagar, G.K., Manickavasagam, L., Singh, S.P., Mishra, G., Wahajuddin, Jain G.K., Maurya, R., Chattopadhyay, N., 2010. A novel flavonoid, 6-C-beta-d-glucopyranosyl-(2S,3S)-(+)-3',4',5,7-tetrahydroxyflavanone, isolated from Ulmus wallichiana Planchon mitigates ovariectomy-induced osteoporosis in rats. Menopause 17 (May-June (3)), 577–586.
Sharma, D.R., Wani, W.Y., Sunkaria, A., Kandimalla, R.J., Verma, D., Cameotra, S.S., Gill, K.D., 2013. Quercetin protects against chronic aluminum-induced oxidative stress and ensuing biochemical, cholinergic, and neurobehavioral impairments in rats. Neurotox. Res. 23 (May (4)), 336–357.
Sharma, D.R., Wani, W.Y., Sunkaria, A., Kandimalla, R.J., Sharma, R.K., Verma, D., Bal, A., Gill, K.D., 2016. Quercetin attenuates neuronal death against aluminum-induced neurodegeneration in the rat hippocampus. Neuroscience 324 (June), 163–176.
Siddiqui, J.A., Sharan, K., Swarnkar, G., Rawat, P., Kumar, M., Manickavasagam, L., Maurya, R., Pierroz, D., Chattopadhyay, N., 2011. Quercetin-6-C-β-D-glucopyranoside isolated from Ulmus wallichiana planchon is more potent than quercetin in inhibiting osteoclastogenesis and mitigating ovariectomy-induced bone loss in rats. Menopause 18 (Febuary (2)), 198–207.
Singh, S., Kumar, S., Dikshit, M., 2010. Involvement of the mitochondrial apoptotic pathway and nitric oxide synthase in dopaminergic neuronal death induced by 6-hydroxydopamine and lipopolysaccharide. Redox Rep. 15, 115–122.
Singh, S., Goswami, P., Swarnkar, S., Singh, S.P., Wahajuddin, Nath, C., Sharma, S., 2011. A study to evaluate the effect of nono tropic drug-piracetam on DNA damage in leukocytes and macrophages. Mutat. Res. 726, 66–74.
Stankov-Jovanović, V.P., Ilić, M.D., Mitić, V.D., Mihajilov-Krstev, T.M., Simonović, S.R., NikolićMandić, S.D., Tabet, J.C., Cole, R.B., 2015. Ecodary metabolites of Seselirigidum: chemical composition plus antioxidant, antimicrobial and cholinesterase inhibition activity. J. Pharm. Biomed. Anal. 111, 78–90.
Swarnkar, G., Sharan, K., Siddiqui, J.A., Chakravarti, B., Rawat, P., Kumar, M., Arya, K.R., Maurya, R., Chattopadhyay, N., 2011. A novel flavonoid isolated from the steam-bark of Ulmus wallichiana planchon stimulates osteoblast function and inhibits osteoclast and adipocyte differentiation. Eur. J. Pharmacol. 658 (May (2-3)), 65–73.
Syed, A.A., Lahiri, S., Mohan, D., Valicherla, G.R., Gupta, A.P., Riyazuddin, M., Kumar, S., Maurya, R., Hanif, K., Gayen, J.R., 2016. Evaluation of anti-hypertensive activity of Ulmus wallichiana extract and fraction in SHR, DOCA-salt- and L-NAME-induced hypertensive rats. J. Ethnopharmacol. 193 (December), 555–565.
Thakare, V.N., Dhakane, V.D., Patel, B.M., 2016. POtential antidepressant-like activity of silymarin in the acute restraint stress in mice: modulation of corticosterone and oxidative stress response in cerebral cortex and hippocampus. Pharmacol. Rep. 68 (October (5)), 1020–1027.
Vauzour, D., Vafeiadou, K., Rodriguez-Mateos, A., Rendeiro, C., Spencer, J.P., 2008. The neuroprotective potential of flavonoids: a multiplicity of effects. Genes Nutr. 115–126.
Velagapudi, R., El-Bakoush, A., Olajide, O.A., 2018. Activation of Nrf2 pathway contributes to neuroprotection by the dietary flavonoid tiliroside. Mol. Neurobiol. (March).
Venigalla, M., Gyengesi, E., Münch, G., 2015. Curcumin and Apigenin - novel and promising therapeutics against chronic neuroinflammation in Alzheimer's disease. Neural Regen. Res. 10 (August (8)), 1181–1185.
Venkatesan, R.S., Sadiq, A.M., 2017. Effect of morin-5'-sulfonic acid sodium salt on the expression of apoptosis related proteins caspase 3, Bax and Bcl 2 due to the mercury induced oxidative stress in albino rats. Biomed. Pharmacother. 85 (January), 202–208.
Verma, D.K., Gupta, S., Biswas, J., Joshi, N., Singh, A., Gupta, P., Tiwari, S., Sivarama Raju, K., Chaturvedi, S., Wahajuddin, M., Singh, S., 2018a. New therapeutic activity of metabolic enhancer piracetam in treatment of neurodegenerative disease: participation of caspase independent death factors, oxidative stress, inflammatory responses and apoptosis. Biochim. Biophys. Acta 1864 (June (6 PtA)), 2078–2096.
Verma, D.K., Gupta, S., Biswas, J., Joshi, N., Sivarama Raju, K., Wahajuddin, M., Singh, S., 2018b. Metabolic enhancer piracetam attenuates the translocation of mitochondrion-specific proteins of caspase-independent pathway, poly [ADP-Ribose] polymerase 1 up-regulation and oxidative DNA fragmentation. Neurotox. Res. 34 (August (2)), 198–219.
Wang, Y., Miao, Y., Mir, A.Z., Cheng, L., Wang, L., Zhao, L., Cui, Q., Zhao, W., Wang, H., 2016. Inhibition of beta-amyloid-induced neurotoxicity by pinocembrin through Nrf2/HO-1 pathway in SH-SY5Y cells. J. Neurol. Sci. 368 (September), 223–230.
Wang, C.P., Shi, Y.W., Tang, M., Zhang, X.C., Gu, Y., Liang, X.M., Wang, Z.W., Ding, F., 2017. Isoquercetin ameliorates cerebral impairment in focal ischemia through antioxidative, anti-inflammatory, and anti-apoptotic effects in primary culture of rat hippocampal neurons and hippocampal CA1 region of rats. Mol. Neurobiol. 54 (April (3)), 2126–2142.
Winklhofer, K.F., Haass, C., 2010. Mitochondial dysfunction in Parkinson's disease. Biochim. Biophys. Acta 1802, 29–44.
Wroblewski, F., Ladue, J.S., 1955. Lactic dehydrogenase activity in blood. Proc. Soc. Exp. Biol. Med. 90, 210–213.